First-principles studies of Au(100)-hex reconstruction in an electrochemical environment

Y. J. Feng,[1] K. P. Bohnen,[2] and C. T. Chan[1]
[1]*Department of Physics, Hong Kong University of Science and Technology, Clear Water Bay, Hong Kong, China*
[2]*Forschungszentrum Karlsruhe, Institut für Festkörperphysik, P.O. Box 3640, D-76021 Karlsruhe, Germany*
(Received 10 April 2005; published 1 September 2005)

Surface energies of Au(100) $p(1\times1)$ and Au(100)-hex as modeled by a $p(1\times5)$ unit cell have been calculated as a function of surface charge by the density functional method. When the surface is neutral, the surface energy of Au(100)-hex is lower than that of Au(100), consistent with the experimental observation that a Au(100) surface has a hexagonal, instead of a square top layer. Calculations show that the surface energies of both systems increase when the surfaces are positively charged and there is a crossover with increasing charge so that the Au(100)-square becomes the ground state. This suggests that the surface-to-hexagonal reconstruction observed in this material can be reversed by an external field or surface charging. The required electric field is quite large, but is achievable at metal/electrolyte interfaces. In this paper, we analyze metal/electrolyte interfacial energies and metal surface energies, discuss the possible role of specific adsorption, and compare our results to experiments by converting the calculated surface energies from surface-charge-density dependent to electrode-potential dependent, based on the relationship of the work function and potential of zero charge. Experimental results can be explained to some extent.

DOI: 10.1103/PhysRevB.72.125401 PACS number(s): 68.35.Bs, 68.08.De, 73.30.+y

I. INTRODUCTION

The ground-state structure of a Au(100) surface consists of a single hexagonal close-packed overlayer on the top of a square array that is the truncated (100) surface of a fcc crystal. This rather special hexagonal reconstructed "Au(100)-hex" surface has been extensively studied. Early low-energy electron diffraction (LEED)[1] and helium diffraction[2] showed a (1×5) reconstruction. Later, more detailed LEED[3] experiments indicated a (20×15) surface structure, and further LEED[4,5] experiments then suggested a $c(26\times68)$ reconstruction. More complicated surface structures have been observed through scanning tunneling microscopy (STM).[6] Several theoretical formulations, including tight binding,[7] a glue model,[8] the embedded atom method,[9] and first-principles total energy calculations together with a Frenkel-Kontorowa model[10] have been applied in an attempt to explain the above structures.

It is interesting to note that the ground-state surface structure can be changed reversibly in an electrochemical environment. Kolb *et al.* have shown that in 0.01M $HClO_4$ solution, Au(100)-hex is stable up to +0.55 V. When the potential increases to a level higher than +0.55 V, Au(100)-hex changes to unreconstructed Au(100). If the gold electrode potential decreases from above +0.55 V to −0.35 V, Au(100) changes back to reconstructed Au(100)-hex. The reconstruction is reversible.[11–14] In this system, the potential of zero charge (PZC) for Au(100)-hex and Au(100) are +0.30 V and +0.08 V with reference to the saturated calomel electrode (SCE), respectively.

Ross *et al.*[15] have analyzed the electric double layer capacitance and the metal/electrolyte interfacial tension under the influence of the electrode potential to see if the electric field (surface charging) or impurity adsorption on the metal surface caused the reversible surface reconstruction. They found that the electrocapillary curves of Au(100)-hex and Au(100) did not cross over, so there should be no surface reconstruction happening within the electrode potential regime in which the surface reconstruction was observed.

To date, the most accurate study of the energetics of this system has employed the local density-functional formalism. Bohnen *et al.* used a first-principles local-density-functional method to study the change of surface energy as a function of surface charging and potential.[16] Due to the complexity of the Au(100)-hex surface, it was simulated by $p(1\times1)$ Au(111). In order to compare theoretical and experimental results, surface charge densities were converted to electrode potentials by integrating an experimental $C(V)$ curve (where C is the differential capacitance of the metal/electrolyte interface, and V is the electrode potential). The surface energy of neutral Au(111) was found to be about 0.2 J/m^2 lower than that of Au(100). Since the results showed that the Au(111) surface energy-potential curve was always below that of Au(100), they concluded that the reconstruction was driven by chemical adsorption rather than by surface charging.

We decided to reconsider this complex system using density-functional calculations for three reasons. First, $p(1\times1)$ Au(111), a truncated (111) surface, may not be a good representation of the Au(100)-hex system, which is an overlayer of close-packed atoms on a truncated (100) surface. A more sophisticated model was adopted to emulate the Au(100)-hex structure. Second, it turns out that the calculations of surface energies in the presence of surface charging involve some subtleties. The concave parabolic nature of the surface energy curves seen in most calculations[16,17] indicates that the electric field energy of the vacuum has been included in the calculations. This quantity, however, is unit-cell-size dependent, and great care must be taken when different orientations are involved. Third, both local-density approximation (LDA) and generalized gradient approximation (GGA) are considered to access the influence of local-density ap-

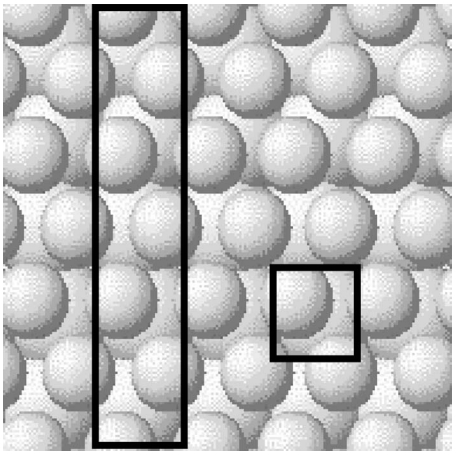

FIG. 1. A schematic plot of the Au(100)-hex surface. The top layer is in reconstructed hexagonal structure. The substrate shows a truncated Au(100) bulk surface. The rectangle and the square show the $p(1\times5)$ Au(100)-hex surface unit cell and the $p(1\times1)$ truncated Au(100) surface unit cell, respectively.

proximation as manifested in different exchange-correlation potentials being used.

II. CALCULATION METHODS

A standard slab model was used to simulate the gold surfaces. In order to avoid systematic errors from the vacuum-electric-field energy, the surface energy λ per unit area in the electric field was defined as

$$\lambda = \frac{1}{2A}\left(\xi_{\text{total}} - n \times \xi_{\text{bulk}} - \frac{1}{8\pi}\int E^2 dv\right), \tag{1}$$

where n is the number of gold atoms in a slab unit cell, ξ_{total} the total energy of the slab, ξ_{bulk} the cohesive energy per atom of fcc gold, A the surface area of the slab, and E the electric field strength. Each slab has two surfaces, hence the factor of $\frac{1}{2}$. In a metallic system, the electric field cannot penetrate the bulk, thus the last term serves to subtract out the vacuum-electric-field energy.

Au(100)-hex, with a hexagonal layer on top of a square network, is a very complex surface system which defies brute force modeling. The smallest commensurate unit cell that can mimic a hexagonal layer on top of a square one is a $p(1\times5)$ surface model,[9] as shown in Fig. 1. The two outermost layers, symmetrically placed on opposite sides of the gold (100) truncated slab, are hexagonal and have 20% more atoms than a truncated Au(100) layer. The inner layers of the slab are bulk fcc in the (100) orientation.

The total energy and force calculations were based on a plane-wave pseudopotential formalism as implemented in a popular program[18] with some modification for the imposition of an electric field. Vanderbilt-type ultrasoft (US) pseudopotentials[19,20] (PP) were applied, with LDA (Ceperley-Alder[21]) and GGA [PW91 (Ref. 22) and PBE (Ref. 23)] exchange-correlation functionals. Comparing the results of previous theoretical calculations[24] with experiment has shown that neither LDA nor GGA is preferred for describing gold, so both LDA and GGA were applied in this study. The projector augmented wave (PAW) potential[25,26] was also tested for the zero-field cases.

The lattice constant and the cohesive energy were calculated using a standard fcc primitive unit cell with a $(20\times20\times20)$ k-point grid. The Au lattice constant was relaxed until the pressure in the unit cell was less than 0.1 kbar, which allowed the cohesive energy ξ_{bulk} to converge to within 0.01 meV. The relaxed lattice constant was then used to construct gold surfaces using a periodic slab model with 11 atomic layers and a 20 Å vacuum. In order to obtain the best cancellation of errors between Au(100)-hex and Au(100), the same $p(1\times5)$ unit cell was used for the Au(100) as for the Au(100)-hex. In both cases, k points were sampled on a (20×4) uniform grid in the two-dimensional (2D) Brillouin zone.[27] For reference, the Au(111) surface energy was calculated as well using a $p(1\times1)$ unit cell with a (20×20) surface k-point grid. In the slab calculations, the unit-cell shape and size were fixed. All atom positions were fully relaxed until the maximum magnitude of force acting on each atom became less than 0.02 eV/Å, such that the atomic positions differed by less than 0.001 Å between the last two relaxation steps. The above procedures guaranteed that the total energy of the slab converged to within 1 meV per unit cell.

III. RESULTS AND DISCUSSION

The calculated lattice constants, cohesive energies, surface energies, work functions, and related theoretical[28–31] and experimental[32–35,15] reference data from other groups are listed in Table I.

The results are in good agreement with previous calculations. Table I shows that the GGA (PW91 and PBE) give lower surface energies than LDA, and this is related to the smaller bulk cohesive energy. For 5d metals, LDA tends to overbind, while GGA underbinds. The results show that the Au(100)-hex surface, as modeled by a commensurate $p(1\times5)$ unit cell, has a lower surface energy than the unreconstructed $p(1\times1)$ Au(100). Au(111) is lower than Au(100), as expected, and Au(100)-hex is in between, with surface energy closer to Au(100) than to Au(111). This is actually the first *ab initio* calculation of the Au(100)-hex surface using a realistic model unit cell that puts a hexagonal layer on top of a square lattice. Both Au(100)-hex and Au(111) are known to have a hexagonal top layer, and the close-packing arrangement is the preferred structure of a 2D layer of Au. However, the Au(111) is commensurate with the truncated bulk, while the Au(100)-hex system has to pay a price for the mismatch between the contracted hexagonal top layer and the (100) substrate layers. The result is that the surface energy of Au(100)-hex is lower than that of Au(100) (due to energy gain from the top layer contraction) but higher than that of Au(111) (due to the lattice mismatch with the bulk). Note that on fcc (100) surfaces, the massive reconstruction of the top layer to a close-packed hexagonal layer is an exception rather than the rule. For example, it does not occur on Ag(100).

TABLE I. Lattice constant a (Å), cohesive energy ξ_{bulk} (eV), surface energy $\lambda(\text{J/m}^2)$ at zero-electric field, and work function Φ (eV) of Au(100), Au(100)-hex, and Au(111).

Method	Reference	a	ξ_{bulk}	$\lambda^{(100)}$	$\lambda^{(\text{hex})}$	$\lambda^{(111)}$	$\Phi^{(100)}$	$\Phi^{(\text{hex})}$	$\Phi^{(111)}$
USPP-LDA	This work	4.06	4.39	1.33	1.32	1.13	5.45	5.50	5.52
USPP-PW91	This work	4.18	3.20	0.85	0.80	0.70	5.11	5.22	5.18
PAW-PBE	This work	4.17	3.27	0.86	0.80	0.70	5.08	5.17	5.14
PP-LDA	10			1.33					
FLAPW-LDA	28	4.065		1.30			5.39		
PP-LDA	29						5.48		5.56
USPP-PBE	30	4.15	3.06	0.90		0.72			
USPP-PBE	31	4.156	3.20			0.820			
Experiment	32	4.08	3.81						
Experiment	33			1.54					
Experiment	34							5.22	5.26
Experiment	35							5.47	5.31
Experiment	15							5.35	5.40

As a check, exactly the same procedure was used to calculate the surface energies of Ag, which is isoelectronic with Au. The surface energy (LDA) of Ag(100)-hex was calculated to be 1.47 J/m^2, which is 0.21 J/m^2 higher than that of $p(1\times1)$ Ag(100), which was found to be 1.26 J/m^2. In Ag, the energy gain from hexagonal contraction is not large enough to overcome the mismatch between the top two surface layers. The calculated results are thus consistent with experiment, in that Au(100)'s top layer tends to become hexagonal, while no reconstructed hexagonal structure is observed on clean Ag(100) surfaces.

Once the metal-surface energy λ is known, the Helmholtz-Perrin equation [Eq. (2)] can be applied to see how the metal/electrolyte interfacial tension γ is changed in an electrochemical environment. In this electrochemical equation, V, V_0, C_0, and γ_0 are the electrode potential, the PZC, the electric double-layer capacitance at the PZC, and the interfacial tension at the PZC, respectively.

$$\gamma-\gamma_0=-\int_{V_0}^{V}dV\int_{V_0}^{V}C\,dV\doteq-\frac{C_0}{2}(V-V_0)^2. \qquad (2)$$

The interfacial tension γ appears to be approximately parabolic, and its peak is at the PZC.

Note that the definition of interfacial tension γ is not the same as the metal-surface energy λ as defined in Eq. (1). Interfacial tension is a complex energy term which involves the metal-surface energy, the electric-field energy in the electric double layer, the interaction energy between the metal and the molecules in the electrolyte, and probably other factors, while the metal-surface energy is the reversible work of formation of a unit area of new metal surface by cleavage in vacuum. At the PZC, there is no excess surface charge and no surface reconstruction; the interfacial tension is equal to the Au surface Helmholtz energy per unit area.[36] In the calculations, the temperature was taken to be 0 K. The contribution of entropy was not considered, so $\gamma_0=\lambda_0$,[37] and Eq. (2) may be rewritten as

$$\gamma=\lambda_0-\int_{V_0}^{V}dV\int_{V_0}^{V}C\,dV. \qquad (3)$$

As long as the capacitance-potential curves are known (measured experimentally, for example), interfacial tension can be plotted against electrode potential using Eq. (3), the calculated gold surface energies, and the experimentally determined capacitance-potential curves.[13]

Figure 2 shows that the interfacial tensions of Au(100) and Au(100)-hex intersect at around 0.36 V (LDA) and 0.70 V (GGA). Experimental observations have shown that the reconstruction happens at 0.55 V.[13,14] Earlier applications of the Helmholtz-Perrin equation to the Au(100)-hex reconstruction (see, for example, Ross *et al.*[15]) were based on tight-binding calculations which estimated the surface-energy difference between the Au(100)-hex and the Au(100) $p(1\times1)$ to be more than 0.2 J/m^2. With such a large surface-energy difference, the capacitance measured in the experiment would not be large enough to drive the reconstruction from (hex) back to $p(1\times1)$. However, Gao and co-workers have noted[38] that the measured electric-double-layer capaci-

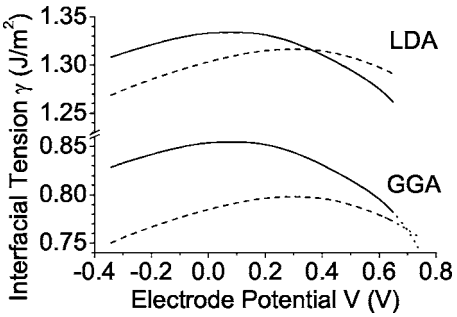

FIG. 2. Interfacial tension at gold/electrolyte interfaces. Solid lines are for Au(100)/$HClO_4$; dashed lines are for Au(100)-hex/$HClO_4$. Dotted lines in the GGA group are an extrapolation of Eq. (3) from experimental capacitance-potential curves.

tance should be accurate, and that it is consistent with potential-induced reconstruction if the surface-energy difference between the Au(100)-hex and the Au(100) $p(1\times1)$ is on the order of 0.02 to 0.03 J/m^2. The density-functional calculations show that this is indeed the case. As shown in Table I, the calculated surface energy of the Au(100)-hex is 0.01 J/m^2 (LDA) or 0.05 J/m^2 (GGA) lower than that of Au(100) $p(1\times1)$. The difference is significantly smaller than that between Au(111) and Au(100): 0.20 J/m^2 (LDA) or 0.15 J/m^2 (GGA). The results so far indicate that the surface-energy difference between the Au(100)-hex and Au(100) $p(1\times1)$ is small, so it is consistent with the capacitance measured in the potential-induced morphology change. However, this does not reveal whether the reversible surface reconstruction is predominantly driven by excess surface charge on the gold surface, by the specific adsorption of ions on gold, or if both factors are important. In order to have a better understanding of the problem, the change in surface energy of gold under the influence of an external imposed electric field was calculated.

The electric field was imposed in the same way as those of Fu and Ho,[17] Bohnen and Kolb,[16] and Che and Chan.[39] A classic charge sheet with a given surface charge density was placed in the middle of the vacuum region. The system is periodic, so the effect is that two charge sheets with a same sign are placed on either side of each Au slab. Electrons were added to or subtracted from the Au slab so as to keep the entire unit cell neutral. During the iteration to self-consistency, the electronic charge within the Au slab was rearranged so as to screen out the external electric field caused by the charge sheet in the vacuum. When self-consistency is reached, the field in the vacuum will be that given by Gauss's Law and as dictated by the charge density of the charge sheet. There will be a layer of surface charge with the sign opposite to that of the imposed charge sheet on the Au surface, and the surface charge density will be one-half that of the externally imposed charge sheet. This surface charge will thus screen the interior of the Au slab from the outside electric field, as it must, since metal does not allow external fields to penetrate. The field can hardly penetrate the top one or two layers for good metals, so a slab of about 11 layers should be thick enough. Note that an electric field can also be imposed by setting up a positive charge sheet on one side and a negative charge sheet on the other side of the slab, which will give the same physics in the case of metallic surfaces. However, imposing symmetrical electric fields has two advantages over asymmetrical positive and negative charge sheets. The symmetrical configuration exhibits more stable convergence toward self-consistency, while the asymmetrical configuration frequently has difficulty in achieving self-consistency due to serious charge sloshing, especially if the slab is thick. In addition, the symmetrical configuration allows for the imposition of a much larger field if the artificial charge sheet is negative (surface positively charged or a depletion of electrons). In the asymmetric configuration, the sign of the electric field on either side of the slab has to be opposite. When a strong field is imposed, the side of the slab that has excess electrons will emit electrons, and the electrons will accumulate in the vacuum around the artificial positive charge sheet. This will not happen with a symmetric

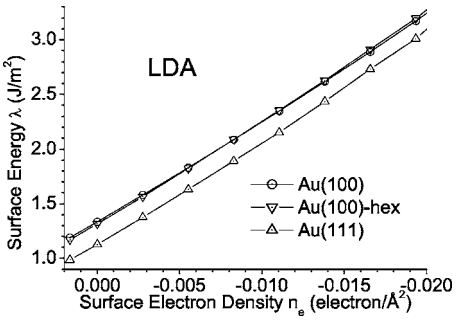

FIG. 3. The surface energy of Au(100) $p(1\times1)$, Au(100)-hex, and Au(111) in an electric field, calculated with the LDA exchange-correlation functional, as a function of the excess surface electron density.

configuration when there is a lack of electrons on the metal surface. This is important, since the field is typically very strong in an electrochemical environment.

In calculating the surface energy under an imposed electric field, the surface energy λ was defined as in Eq. (1). Note that other studies[17,16] have calculated the surface energy in the presence of surface charging using

$$\lambda = \frac{1}{2A}(\xi_{\text{total}} - n \times \xi_{\text{bulk}}). \tag{4}$$

They have thus included the field energy of the vacuum into the surface energy of the system. The surface energy would then depend on the unit cell chosen, since the vacuum field energy increases with the size of the vacuum region. This is fine as long as consideration is confined to the energetics of one orientation using the same unit cell, since the vacuum field energy will be subtracted off when energy differences are calculated. However, when the surface energies of different orientations are considered, it is much safer to subtract the vacuum energy, so calculated quantities do not depend on the unit cell chosen. Note that in the electrochemical environment, there is electrostatic energy stored in the electric double layer, which has a thickness that is typically measured in angstroms. However, the capacitance energy stored in the electric double layer depends on the details of the ions and the electrolytes and, in general, does not bear any relationship to the vacuum field energy in the supercell calculation.

Calculated values of λ, as defined in Eq. (1), are given in Fig. 3. Figure 3 was calculated using the LDA approach, but the qualitative behavior is the same when the results are calculated with GGA-PW91. The surface energies increase with surface-charge density ($\sigma=-n_e e$) and have an almost linear dependence on the field strength. The surface energy of Au(111) is substantially lower than that of Au(100) $p(1\times1)$, hence the effect of the electric field cannot switch the order of these two surfaces. Note that these results differ from those of Bohnen *et al.*[16] They found that there is a crossover between Au(111) and Au(100) $p(1\times1)$, which can be traced to their inclusion of a unit-cell-dependent vacuum-field term in their calculations. However, the surface-energy

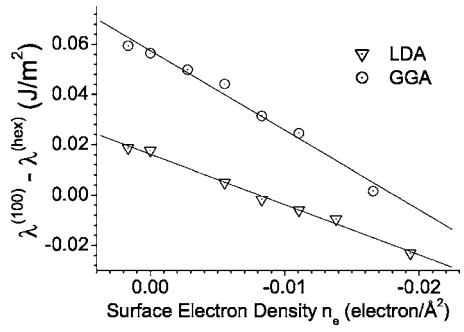

FIG. 4. The surface energy difference of Au(100) $p(1\times1)$ and Au(100)-hex, calculated with LDA (triangles) and GGA (circles), as a function of the excess surface electron density.

difference between Au(100) and the Au(100)-hex is much smaller, such that surface charging can indeed switch the order.

Figure 4 shows that the Au(100)-hex is more stable in neutral conditions, but Au(100) $p(1\times1)$ becomes more stable when the surface is positively charged. This can be understood by considering that as far as a metal is concerned, the existence of an external electric field and excess surface charge imply on each other, so that the surface-energy change induced by the external field can be understood by adding electrons to (or taking them from) the surface. As noted by Monnier *et al.*,[40]

$$d\lambda = \mu_e dn_e = -\frac{1}{e}\mu_e d\sigma. \tag{5}$$

So, the first-order term of a Taylor expansion of $\lambda(\sigma)$ is contributed by

$$\left.\frac{d\lambda}{d\sigma}\right|_{\sigma=0} = -\frac{\mu_{e(\sigma=0)}}{e} = \frac{\Phi}{e}. \tag{6}$$

The work function Φ is defined as $\Phi = V_{\text{vac}} - \mu_e$, where μ_e is the electrochemical potential of the electron for the specific surface, and V_{vac} is the potential energy of the electron in the vacuum far away from the surface. V_{vac} is taken to be zero in our consideration, thus $\Phi = -\mu_e$. The work function of a specific surface depends on the electron energy necessary to penetrate the dipole barrier at the surface, and the bulk electrochemical potential of the electron relative to the mean electrostatic potential in the metal interior.[41] Since the slope of $\lambda(\sigma)$ is related to the work function of the surface in linear order, the work function has been calculated to see if the results are consistent with the surface-energy change.

The $V_{\text{local}}^{\text{ion}} + V_{\text{Hartree}}$ potential was calculated along the direction perpendicular to the slab to get the work function of the specific surface.[42] As shown in Table I, $\Phi^{(\text{hex})}$ was indeed higher than $\Phi^{(100)}$, consistent with the results that $\lambda(\sigma)$ has a larger positive slope for Au(100)-hex than for Au(100) $p(1\times1)$. Because the difference between $\lambda^{(\text{hex})}$ and $\lambda^{(100)}$ at zero field is rather small, the difference in the slope of $\lambda(\sigma)$ is sufficient to cause a crossover so that Au(100)-hex becomes higher in energy than Au(100) in the relevant range of σ. The critical surface charge densities calculated using LDA and GGA were -0.0097 e/Å^2 and -0.0158 e/Å^2, corresponding to an electric field of 1.8 V/Å and 2.9 V/Å, respectively. We thus conclude that for a clean Au(100) surface, the surface reconstruction between (hex) and $p(1\times1)$ can be induced by an external field or surface charging. At the same time, we note that Au(111) is not a good substitute for the Au(100)-hex in this analysis. Au(111) has a surface energy that is significantly lower than that of Au(100), and the results are rather different from those for Au(100)-hex. In fact, Au(111) will remain lower in surface energy than Au(100) $p(1\times1)$ over the entire range of electric-field strengths or surface charges under consideration.

Making a direct comparison with the experiment involves overcoming two major complications. The first is that the experiment is done at a given voltage, not a given external field. The second is that the Au surface is submerged in the electrolyte, and the adsorption of electrolyte ions on the surface can change the surface properties. In principle, both of these issues can be dealt with through local-density-functional calculations if we can afford to treat the complete metal/electrolyte interface—not just the Au surface, but also the anion adsorption, the effect of water, and the properties of the electric double layer. Due to limited resources, however, it is difficult to reflect all of these influences in a complete *ab initio* manner.

First, we try to change the external parameter from field to voltage. It quickly becomes apparent that the conversion requires knowledge of the capacitance of the surface system. To compare surface energies at a particular electrode potential, expand $\lambda(V)$ at potential of zero-charge V_0. Assume at first that the effects of specific adsorption can be ignored. From the Gouy-Chapman theory,[43] $dC/dV = 0$ at PZC, thus, the first and the second derivatives of λ are, respectively,

$$\lambda_0' = \left[\frac{d\lambda}{d\sigma}\frac{d\sigma}{dV}\right]_0 = C_0\frac{\Phi}{e}, \tag{7}$$

$$\lambda_0'' = \left[C\frac{d}{dV}\left(\frac{d\lambda}{d\sigma}\right)\right]_0 = \left[C\frac{d}{d\sigma}\left(\frac{d\lambda}{d\sigma}\right)\frac{d\sigma}{dV}\right]_0 = C_0^2\left(\frac{d^2\lambda}{d\sigma^2}\right)_0. \tag{8}$$

Truncating the Taylor expansion of $\lambda(V)$ beyond the first three terms yields

$$\lambda(V) \doteq \lambda_0 + C_0\frac{\Phi}{e}(V - V_0) + \frac{1}{2}\left(\frac{d^2\lambda}{d\sigma^2}\right)_0 [C_0(V - V_0)]^2. \tag{9}$$

The potential of zero charge and the work function of a metal surface are related by[44,45]

$$V_0^{(hkl)} = \Phi^{(hkl)}/e + \delta\chi_M^{(hkl)} + g_S^{(hkl)} + K. \tag{10}$$

$\delta\chi_M^{(hkl)}$ is from the change of the metal surface dipole when it is in contact with the electrolyte; $g_S^{(hkl)}$ is due to the reorientation of electrolyte dipoles at the metal/electrolyte interface; and K is the potential drop at the reference electrode. K is a constant for a particular reference electrode. Assuming there is no specific adsorption and that the system satisfies the Gouy-Chapman approximation, the influence of $\delta\chi_M^{(hkl)}$ and

$g_S^{(hkl)}$ on different surface orientations should be small enough to neglect. $\Delta|\delta\chi_M^{(hkl)}+g_S^{(hkl)}|\doteq 0$. Then

$$V_0^{(\mathrm{hex})} - V_0^{(100)} \doteq [\Phi^{(\mathrm{hex})} - \Phi^{(100)}]/e. \quad (11)$$

Letting $U=V-V_0^{(100)}$ and $\Delta\Phi/e=[\Phi^{(\mathrm{hex})}-\Phi^{(100)}]/e$, we get

$$\lambda^{(100)}(U) = \lambda_0^{(100)} + C_0^{(100)}\frac{\Phi^{(100)}}{e}U + \frac{1}{2}\left(\frac{d^2\lambda^{(100)}}{d\sigma^2}\right)_0 (C_0^{(100)}U)^2, \quad (12)$$

$$\lambda^{(\mathrm{hex})}(U) = \lambda_0^{(\mathrm{hex})} + C_0^{(\mathrm{hex})}\frac{\Phi^{(\mathrm{hex})}}{e}(U-\Delta\Phi/e) + \frac{1}{2}\left(\frac{d^2\lambda^{(\mathrm{hex})}}{d\sigma^2}\right)_0 [C_0^{(\mathrm{hex})}(U-\Delta\Phi/e)]^2. \quad (13)$$

Equations (12) and (13) are written in a form such that most of the variables can be calculated using a local-density-functional formalism, except C_0. It was not possible to calculate a metal/electrolyte interface with electrolyte molecules in this study due to limited computing resources.[46] To proceed any further required using a C_0 determined experimentally.

Figure 5 is based on theoretical $\lambda(\sigma)$ values calculated according to the LDA and GGA-PW91. $C_0^{(100)}$ was taken to be 20 μF/cm^2, and $C_0^{(\mathrm{hex})}$ was taken to be 26 μF/cm^2.[16] Figure 4 shows that surface charging (or a positive external field) can drive the transition between Au(100)-hex and Au(100) $p(1\times 1)$. Figure 5 shows that if an experimental capacitance value is used to convert λ from charge dependent to potential dependent, the Au(100) surface reconstruction is reversible at a certain electrode potential. The calculated critical potential is 0.35 V (LDA), or 0.68 V (GGA) with reference to SCE, which is consistent with the previous analysis of interfacial tension.

One may ask why use Eq. (11) and the work function difference from the calculations (0.052 eV LDA, 0.11 eV PW91, and 0.094 eV PBE) instead of using the PZC difference (0.22 V) measured by experiment. The reason is that there are several pieces of evidence showing that there is ion adsorption on metal surfaces in similar electrochemical systems.[47] This would not significantly affect the metal-surface structure, but would shift the transition potential. Since the adsorption details are unknown, it is difficult to model such systems in theoretical calculations. Moreover, the objective is to understand how the transition happens when surface energies of gold change in response to an electrode potential, so it is appropriate to focus on the surface energies of pure gold. In more precise terms, Eqs. (12) and (13), and hence Fig. 5, are treating the energetics of a Au/vacuum interface under an external potential, with the capacitance taken from that measured in an electrochemical environment and the vacuum-electric-field energy subtracted.

It is instructive to compare the work functions calculated through the density functional formalism with experimentally determined work functions and PZC data. Ross and co-workers[15] measured the work functions of clean annealed surfaces in ultrahigh vacuum (UHV). They then immersed the surfaces in 0.01M $HClO_4$ and measured the work functions again when the surfaces emerged from the electrolyte at their respective PZCs. For Au(111) and Au(100)-hex, the measured work function difference between the clean annealed Au(111) and the clean annealed Au(100)-hex was 0.05 ± 0.1 eV, or very small. The work functions of the surfaces after exposure both increase by 0.1 eV compared to the clean annealed values, but the work function difference remained the same, 0.05 ± 0.1 eV. These work function differences for both the clean annealed surfaces and the emerged surfaces are consistent with the PZC difference measured in experiments, 0.05 ± 0.07 V. The theoretical work function difference between Au(111) and Au(100)-hex calculated in this study was 0.016 eV (LDA), −0.048 eV (GGA-PW91), or −0.025 eV (GGA-PBE), in the region of 0.05 ± 0.1 eV. These results show that the work function difference of Au(111) and Au(100)-hex should be very small, which is consistent with experimental measurements.

The experimental work function difference between the emerged Au(100)-hex and the emerged Au(100) is 0.25 ± 0.1 eV. It is consistent with the PZC difference 0.2 ± 0.05 V measured from that experiment. It is also consistent with D. M. Kolb's experimentally measured PZC difference of 0.22 V. However, the theoretical work function difference between the Au(100)-hex and the Au(100) calculated in this study was 0.052 eV (LDA), 0.11 eV (PW91), or 0.094 eV (PBE). These results are significantly smaller than the experimentally measured values for Au(100)-hex and Au(100).

It seems perplexing that the theoretical work function difference calculated for Au(111) and Au(100)-hex is consistent with experiments, but it is not for the case of Au(100)-hex and Au(100). Several pieces of evidence show that impurities may shift the observed transition potential,[47] and, as mentioned by Schmickler and Leiva,[37] adsorption shifts the PZC of the metal surface, and the PZC measured from the electric double-layer capacitance-potential curve may not represent the PZC of a pure metal surface. So, the inconsistency may arise not from the theoretical calculations, but from the experimental work functions of emerged surfaces. When there are ions adsorbed on the surface, the measured PZC should represent the PZC of a metal surface with impurities. The corresponding work function of this PZC should be the work function of a metal surface together with its impurity ions. The work function of the surface can thus be significantly modified by the adsorption of the ions. For the case of the Au(111) and the Au(100)-hex, their surface geometries are quite close to each other, so ion adsorption on these two surfaces could be very similar. When calculating the experimental work function difference or the PZC difference, the influence of ion adsorption could cancel out to a large extent. Therefore, the experimental data seem to be consistent with the theoretical calculations. The surface geometries of Au(100)-hex and Au(100) are quite different—one is hexagonal and the other is square—so the nature of ion adsorption on these two surfaces should also be quite different. The influence of ion adsorption on the work functions (and the PZC values) of the two surfaces could then be different as well. When subtracting the experimentally determined work functions of emerged surfaces, the influence of ion adsorp-

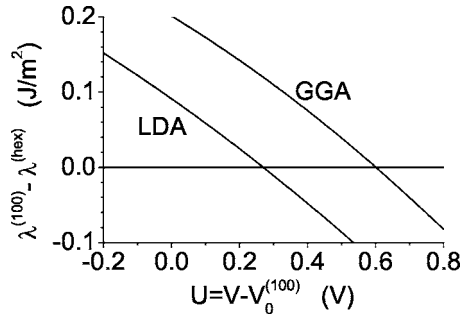

FIG. 5. The surface-energy difference between Au(100) and Au(100)-hex as a function of electrode potential with reference to the PZC of Au(100). ($V_0^{(100)}$=0.08 V with reference to SCE.)

tion may not cancel out. Therefore, theory and experiment might be different for this case. Since adsorption can change the PZC of the surface, and the PZC measured in the experiment corresponds to a contaminated surface, there is no reason to use this PZC difference when analyzing the surface energies of clean metal surfaces.

If experimental PZC values are taken as charge zero points for the clean metal surfaces, the large difference in the experimental PZC values separates the curves for Au(100) and Au(100)-hex from each other to such an extent that no field effect can possibly change the order of these two surfaces.[16] If we consider a metal surface together with its adsorbed ions as a new surface system, the experimental work function and the PZC of this new surface should always be consistent. It would be interesting in the future to calculate the properties of metal surfaces with adsorbed ions in an aqueous environment, and then calculate the surface energies and the work functions of the surfaces in the electrochemical environment.

We would also like to make a remark about Figs. 5 and 2. Figure 5 is the surface-energy difference between different Au surfaces as a function of the external potential. The electrostatic energy of the electric double layer in the electrolyte is not considered. Figure 2 considers the interfacial tension and takes the capacitance energy of the electric double layer and other interaction energies between the metal surface and the solvent molecules into account in an entirely empirical fashion.

IV. SUMMARY

Local-density-functional calculations show that the surface-energy differences between Au(100) $p(1\times1)$ and Au(100)-hex surfaces are very small, at the order of 0.02 J/m^2. This implies that earlier attempts by other authors to emulate the Au(100)-hex surface using Au(111) have actually not been justified, since a Au(111) surface has significantly lower surface energy than that of Au(100) $p(1\times1)$. Taking the surface energies of neutral Au(100)-hex and neutral Au(100) $p(1\times1)$, together with electric double-layer capacitances measured from experiments, calculations show that surface reconstruction is indeed electrode potential induced.

These first-principles calculations have shown that a positive field favors the Au(100) $p(1\times1)$ arrangement, so that if a Au(100) surface is positively charged, it will transform from the (hex) to the $p(1\times1)$ structure. Reversible Au(100)-hex surface reconstruction can be thus induced by surface charging. In order to make connection with the reversible (hex)$\leftrightarrow p(1\times1)$ reconstruction observed in electrochemical environments, it is necessary to convert from surface charging to electrode potential. This requires a knowledge of the capacitances of the system, for which experimental values are available. The results are reasonably close to the result from interfacial tension analysis, and they are also close to experimental observations.

At this stage, there is not sufficient information to tell whether or not ion adsorption plays a key role in governing the observed change of morphology at the electrochemical interface. We can say only that the surface charging induced by an electrode potential (and by the electric double layer at the metal/electrolyte interface) already constitutes a sufficient driving force to cause Au(100)-hex surface reconstruction. A complete picture of the metal/electrolyte interface requires details down to the atomic level, not only on the metal side of the interface but also in the electrolyte. A fully *ab initio* treatment of the electrolyte under an intense field remains a challenge for the foreseeable future.

ACKNOWLEDGMENTS

This work was supported by RGC Hong Kong through Grant No. HKUST6152/01P. Computation resources were supported by an EHIA grant from the Hong Kong University of Science and Technology.

[1] D. G. Fedak and N. A. Gjostein, Phys. Rev. Lett. **16**, 171 (1966).
[2] K. H. Rieder, T. Engel, R. H. Swendsen, and M. Manninen, Surf. Sci. **127**, 223 (1983).
[3] D. G. Fedak and N. A. Gjostein, Surf. Sci. **8**, 77 (1967).
[4] J. F. Wendelken and D. M. Zehner, Surf. Sci. **71**, 178 (1978).
[5] M. A. Van Hove, R. J. Koestner, P. C. Stair, J. P. Biberian, L. L. Kesmodel, I. Bartos, and G. A. Somorjai, Surf. Sci. **103**, 189 (1981); **103**, 218 (1981).
[6] G. K. Binning, H. Rohrer, C. Gerber, and E. Stoll, Surf. Sci. **144**, 321 (1984).
[7] D. Tomanek and K. H. Bennemann, Surf. Sci. **163**, 503 (1985).
[8] F. Ercolessi, E. Tosatti, and M. Parrinello, Phys. Rev. Lett. **57**, 719 (1986).
[9] Brian W. Dodson, Phys. Rev. B **35**, 880 (1987).
[10] Noboru Takeuchi, C. T. Chan, and K. M. Ho, Phys. Rev. B **43**, 14363 (1991).
[11] D. M. Kolb and J. Schneider, Surf. Sci. **162**, 764 (1985).
[12] D. M. Kolb and J. Schneider, Electrochim. Acta **31**, 929 (1986).

[13] J. Schneider and D. M. Kolb, Surf. Sci. **193**, 579 (1988).
[14] D. M. Kolb, Prog. Surf. Sci. **51**, 109 (1996).
[15] Philip N. Ross and Alfred T. D'Agostino, Electrochim. Acta **37**, 615 (1992).
[16] K. P. Bohnen and D. M. Kolb, Surf. Sci. **407**, L629 (1998).
[17] C. L. Fu and K. M. Ho, Phys. Rev. Lett. **63**, 1617 (1989).
[18] G. Kresse and J. Hafner, Phys. Rev. B **47**, R558 (1993); G. Kresse and J. Furthmüller, *ibid.* **54**, 11169 (1996).
[19] D. Vanderbilt, Phys. Rev. B **41**, R7892 (1990).
[20] G. Kresse and J. Hafner, J. Phys.: Condens. Matter **6**, 8245 (1994).
[21] D. M. Ceperley and B. J. Alder, Phys. Rev. Lett. **45**, 566 (1980); J. P. Perdew and A. Zunger, Phys. Rev. B **23**, 5048 (1981).
[22] J. P. Perdew, J. A. Chevary, S. H. Vosko, K. A. Jackson, M. R. Pederson, D. J. Singh, and C. Fiolhais, Phys. Rev. B **46**, 6671 (1992).
[23] J. P. Perdew, K. Burke, and M. Ernzerhof, Phys. Rev. Lett. **77**, 3865 (1996).
[24] A. Khein, D. J. Singh, and C. J. Umrigar, Phys. Rev. B **51**, 4105 (1995).
[25] P. E. Blochl, Phys. Rev. B **50**, 17953 (1994).
[26] G. Kresse and D. Joubert, Phys. Rev. B **59**, 1758 (1999).
[27] H. J. Monkhorst and J. D. Pack, Phys. Rev. B **13**, 5188 (1976).
[28] E. Eibler, H. Erschbaumer, C. Temnitschka, R. Podloucky, and A. J. Freeman, Surf. Sci. **280**, 398 (1993).
[29] C. Sànchez and E. Leiva, Electrochim. Acta **45**, 691 (1999).
[30] T. Hayashi, Y. Morikawa, and H. Nozoye, J. Chem. Phys. **114**, 7615 (2001).
[31] Y. Yourdshadyan and Andrew M. Rappe, J. Chem. Phys. **117**, 825 (2002).
[32] C. Kittel, *Introduction to Solid State Physics*, 7th ed. (Wiley, New York, 1996).
[33] W. R. Tyson and W. A. Miller, Surf. Sci. **62**, 267 (1977).
[34] G. V. Hansson and S. A. Flodström, Phys. Rev. B **18**, 1572 (1978).
[35] H. C. Potter and J. M. Blakely, J. Vac. Sci. Technol. **12**, 635 (1975).
[36] D. H. Everett, Pure Appl. Chem. **31**, 577 (1972); http://www.iupac.org/reports/2001/colloid_2001/manual_of_s_and_t/
[37] W. Schmickler and E. Leiva, J. Electroanal. Chem. **453**, 61 (1998).
[38] Xiaoping Gao, Gregory J. Edens, Antoinette Hamelin, and Michael J. Weaver, Surf. Sci. **296**, 333 (1993).
[39] J. G. Che and C. T. Chan, Phys. Rev. B **67**, 125411 (2003).
[40] R. Monnier, J. P. Perdew, D. C. Langreth, and J. W. Wilkins, Phys. Rev. B **18**, 656 (1978).
[41] E. Wigner and J. Bardeen, Phys. Rev. **48**, 84 (1935).
[42] T. C. Leung, C. L. Kao, W. S. Su, Y. J. Feng, and C. T. Chan, Phys. Rev. B **68**, 195408 (2003).
[43] W. Schmickler, *Interfacial Electrochemistry* (Oxford University Press, New York, 1996); G. Gouy, J. Phys. Theor. Appl. **9**, 457 (1910); D. L. Chapman, Philos. Mag. **25**, 475 (1913).
[44] S. Trasatti, J. Electroanal. Chem. Interfacial Electrochem. **33**, 351 (1971).
[45] J. Lecoeur, J. Andro, and R. Parsons, Surf. Sci. **114**, 320 (1982).
[46] http://www.phys.ust.hk/pccluster
[47] J. Wang, A. J. Davenport, H. S. Isaacs, and B. M. Ocko, Science **255**, 1416 (1992); B. M. Ocko, G. Helgesen, B. Schardt, J. Wang, and A. Hamelin, Phys. Rev. Lett. **69**, 3350 (1992); J. Wang, B. M. Ocko, A. J. Davenport, and H. S. Isaacs, Phys. Rev. B **46**, 10321 (1992); K. Ataka, T. Yotsuyanagi, and M. Osawa, J. Phys. Chem. **100**, 10664 (1996).